nature

https://doi.org/10.1038/s41586-024-07341-z

Accelerated Article Preview

Copper-catalyzed dehydrogenation or lactonization of C(sp^3)–H bonds

Received: 27 September 2023

Accepted: 21 March 2024

Accelerated Article Preview

Cite this article as: Zhou, S. et al. Copper-catalyzed dehydrogenation or lactonization of C(sp^3)–H bonds. *Nature* https://doi.org/10.1038/s41586-024-07341-z (2024)

Shupeng Zhou, Zi-Jun Zhang & Jin-Quan Yu

Copper-catalyzed dehydrogenation or lactonization of C(sp^3)−H bonds

Authors: Shupeng Zhou,[1,†] Zi-Jun Zhang,[1,†] Jin-Quan Yu[1,*]

Affiliations: [1]Department of Chemistry, The Scripps Research Institute, 10550 North Torrey Pines Road, La Jolla, California 92037, United States.

*Correspondence to: yu200@scripps.edu

†These authors contributed equally to this work.

Cytochrome P450 enzymes are known to catalyze bimodal oxidation of aliphatic acids via radical intermediates, which partition between pathways of hydroxylation and desaturation[5,6]. Developing analogous catalytic systems for remote C−H functionalization remains a significant challenge[14,15,16]. Here we report the development of Cu(I)-catalyzed bimodal dehydrogenation/lactonization reactions of synthetically common *N*-methoxyamides via radical abstractions of the γ-aliphatic C−H bonds. The feasibility of switching from dehydrogenation to lactonization has also been demonstrated by altering reaction conditions. The use of a readily available amide as both radical precursor and internal oxidant allowed for the development of a redox-neutral C−H functionalization reactions with methanol as the sole side product. These C−H functionalization reactions using Cu(I) catalyst of loading as low as 0.5 mol% have been applied to the diversification of a wide range of aliphatic acids including drug molecules and natural products. The exceptional compatibility of this catalytic system with a wide

range of oxidatively sensitive functionality demonstrates the unique advantage of using simple amide substrate as the mild internal oxidant.

Main Text: Olefins and carbon-oxygen bonds are ubiquitous and highly important in organic synthesis[1]. A particularly attractive strategy for constructing such moieties is the direct oxidation of inert C−H bonds. The generation of a C−O bond at the expense of a C−H bond leads to increased complexities and enables the direct synthesis of the target of interest from a simple hydrocarbon fragment[2,3]. From the perspective of downstream diversification, the desaturation of aliphatic chains by C−H dehydrogenation can be even more versatile than the direct conversion of C−H to C−O bonds. Nature has evolved various enzymes to catalyze the direct oxidation of hydrocarbon skeletons with great precision[4]. In some cases, a single enzyme was found to simultaneously catalyze different types of reactions[5,6]. In 1987, a landmark discovery by Baillie and coworkers showcased that a type of hepatic cytochrome P450, normally considered a hydroxylase, could also act as a desaturase[5]. It is believed that a common carbon-centered radical intermediate is responsible for this mixed hydroxylase/desaturase activity (Fig. 1a). Inspired by this remarkable enzymatic chemistry, we envisioned the possibility of accessing remote bimodal C−H dehydrogenation/oxygenation reaction with metal catalysts through radical abstraction. Such a reaction could be useful for direct oxidation state elevation of hydrocarbon frameworks[2,3], and it would be a valuable tool for late-stage modifications and diversifications of natural products and drug molecules[7-9]. Although biomimetic dehydrogenation and oxygenation reactions based on the hydrogen atom abstraction strategy have been reported starting with the pioneering work of Breslow[10,11] and Groves[12,13] *et al.*, dual desaturation/oxygenation reaction remains a grand challenge. The few early examples suffered from limited scope (only for benzylic C−H)[14,15] and/or

overoxidation[15,16]. Moreover, these methods require exogenous stoichiometric oxidants, most of which give mixed dehydrogenated/hydroxylated products and cannot be tuned to produce a single major product. Therefore, the development of a controllable bimodal dehydrogenation/oxygenation reaction would be highly desirable.

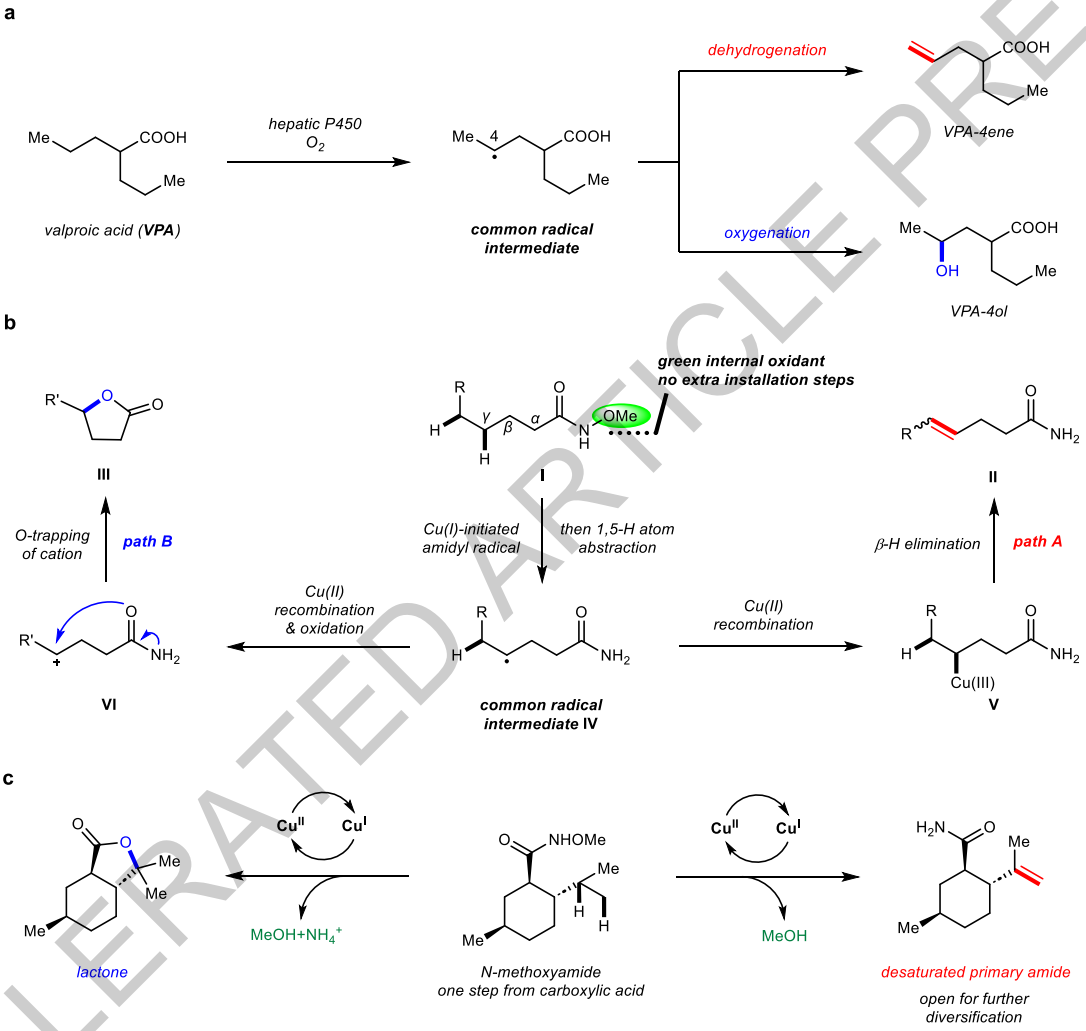

N-methoxyamides have become a major class of practically useful substrates in Pd(II)- and Rh(III)-catalyzed C−H activation reactions[17] since their first introduction[18]. They can be readily prepared in large quantities from carboxylic acids in a single step and are bench-stable for long-term storage. Despite advances

in the field of amidyl radical generation via N−O cleavage[19,20], specifically from activated *O*-acyl and *O*-aryl hydroxamides with photocatalysis[21-24], the simple *N*-methoxyamide substrates have not been shown to be compatible with these chemistry, presumably due to its relatively high reduction potential[25]. Notably, developing C−H functionalization reactions based on such radical abstraction require external traps[20] or photocatalysis of highly redox-active groups[26] to close the redox catalytic cycle. Inspired by previously reported Cu(I)-mediated formation of iminyl radicals from active oxime esters and subsequent cyclization with tethered olefins[27], we wondered whether Cu(I) could reduce *N*-methoxyamides to form amidyl radicals (the efforts to overcome the relatively high BDE of N−O bond of *N*-methoxyamide are summarized in the SI). If successful, this reductive method would essentially use the methoxy group as the green internal oxidant, thus omitting the photoredox catalysts, and external oxidants which often lead to overoxidation. This amidyl radical **I** can then perform 1,5-H atom abstraction to form the *γ*-carbon-centered radical **IV** (Fig. 1b). We envisioned that the combination of this alkyl radical with Cu(II) species could either favor oxidative elimination to afford dehydrogenation products (**V** to **II, path A**) or undergo oxidative substitution leading to the formation of lactone **III** via intramolecular trapping of carbocationic intermediate **VI** (**path B**)[28-30]. In both pathways, Cu(I) would be regenerated, closing this redox-neutral catalytic cycle. The only by-product of the dehydrogenation reaction is MeOH (or MeOH and ammonium salt for the lactonization). Here, we report a redox-neutral Cu-catalyzed bimodal dehydrogenation/lactonization reaction of *N*-methoxyamides without using highly reactive redox-active groups which require additional installation steps. This platform would allow the rapid diversification of widely available carboxylic acids into valuable lactones and

dehydrogenated primary amides (Fig. 1c), where the amides could be further diversified by transformations of the amide, functionalization of the alkene and a cyclization between the amide and the double bond.

To our delight, the realization of the dehydrogenation was enabled by using CuF_2 (10 mol%) as the catalyst, 8-methoxyquinoline (20 mol%) as the ligand, and AcOH as the additive in 1,4-dioxane or DCE (Fig. 2; the details of the reaction optimization are discussed in the SI, see Figure S1-S6). Under these reaction conditions, *N*-methoxyamide **A27** gave dehydrogenated product **B27** in 70% yield.

With the optimized reaction conditions in hand, we began to explore the substrate scope of the dehydrogenation (Fig. 2 and Extended Data Fig. 1). Both unactivated (**A1-A8**) and benzylic (**A9-A25**) γ-C−H bonds reacted to form the corresponding olefins in good yields with both acyclic and cyclic substrates. β,γ-olefins can also be obtained as the major product when the δ-position was blocked **(B4** and **B5**). A particularly striking example is the formation of γ,δ-unsaturated skipped diene **B2** rather than the conjugated β,γ-olefin. We were delighted to find that *N*-methoxyamides bearing *γ*-methines were also competent substrates, affording the desired olefins (**B26-B38**). Although small amounts of β,γ-unsaturated isomers were formed in some cases (**B33-B36**), the reaction generally exhibited a strong preference for the formation of γ,δ- rather than β,γ-olefins. The reaction was also found to tolerate a wide range of functionality, including alkyl acetates (**B3**, **B6**, and **B28**), pre-existing olefins (**B2**, **B20**, and **B26**), alkynes (**B21**), (thio)ethers (**B10**, **B22**, **B24**, and **B25**), carbamates (**B19**), heterocycles (**B11**, **B22**, and **B23**), and potential cross coupling partners for downstream elaborations such as aryl halides (**B13**, **B14**, and **B18**) and boronic esters (**B15**). The exceptional ability of this oxidative catalytic system to tolerate a wide range of oxidatively sensitive

functionality demonstrates the unique advantage of using amide substrate as the mild internal oxidant rather than using harsh exogenous oxidants.

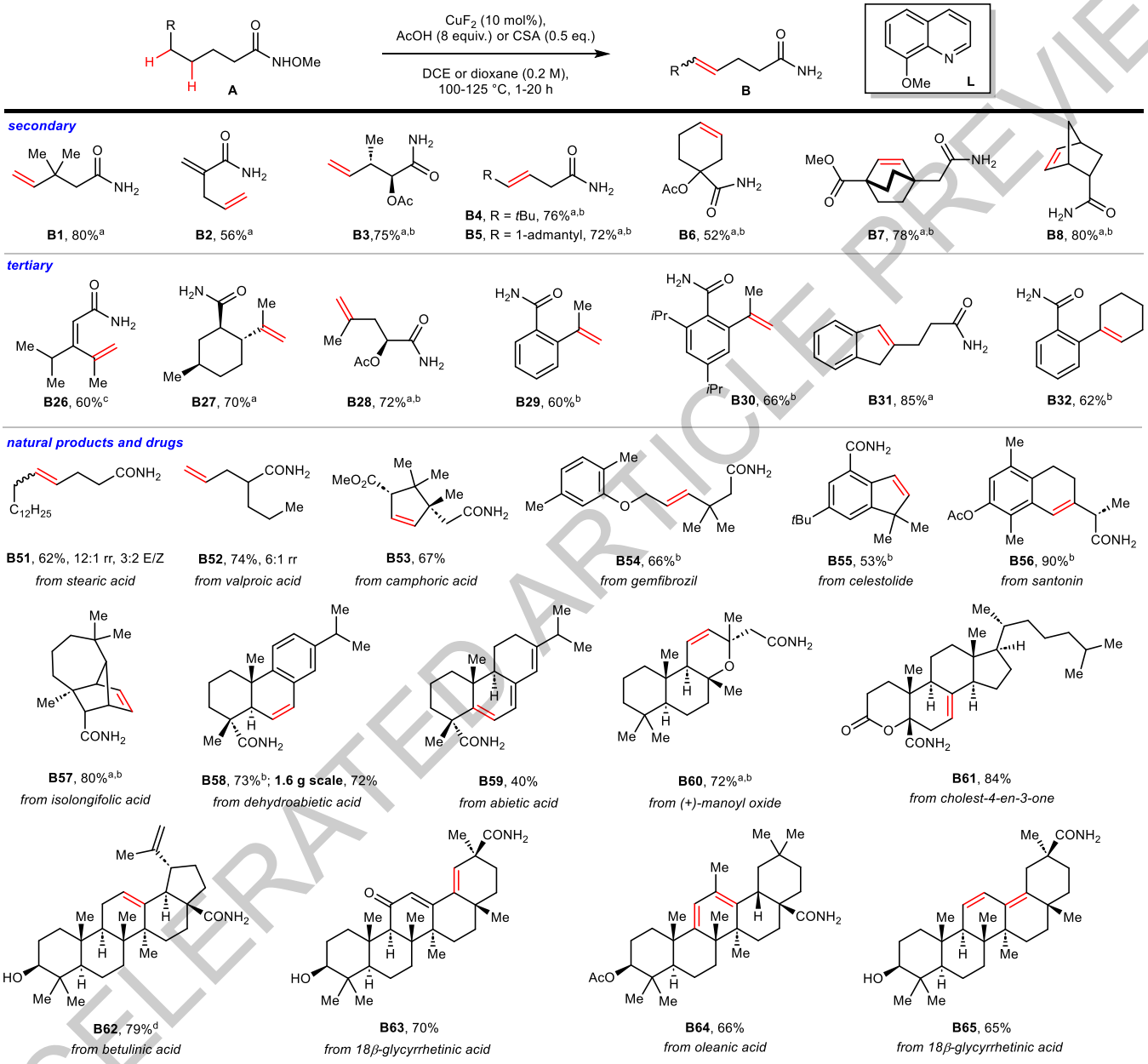

We next examined the reaction in a range of more complex settings. A variety of α-, β-, and γ-amino acid derivatives were subjected to the reaction, affording the corresponding dehydrogenated products in synthetically useful yields (**B39-B50**, Extended Data Fig. 1). *N*-Methoxyamide derivatives of natural

products and pharmaceuticals also proved amenable to dehydrogenation (**B51-B65,** Fig. 2). The exclusive formation of mono-desaturation product **B52** from valproic acid derivative **A52** offers a particularly notable example, as our internal oxidant strategy, unlike the use of external oxidant, prevents further dehydrogenation. Site-selectivity became somewhat more complicated with polycyclic substrates. Betulinic acid derivative **B62** offers a particularly informative example wherein high yields of a single product were obtained despite the presence of four competing γ-C−H bonds. Notably, the major product was formed by HAT at an unactivated methine rather than the allylic γ-methine, indicating that geometric factors can outweigh the intrinsic reactivity of the competing C−H bonds. As with the examples discussed above, the reaction displayed a remarkable tolerance for sensitive functionality such as the conjugated triene system formed in **B59**, though migration of the pre-existing double bond was observed in **B64** and **B65** (see the SI for details). Considering that abietane-type structures are widely found in nature and are also precursors of many complex terpenes, we decided to test a large-scale reaction on the derivative of dehydroabietic acid. Treatment of 1.6 gram of **A58** with CuF_2 (5 mol%) and CSA (0.5 equiv.) gave **B58** in 72% yield after refluxing for 20 hours.

Amidyl radicals can in principle be utilized to synthesize γ-lactones via derivations of the classical Hofmann-Löffler-Freytag reaction[31-35], but both the multiple-step reaction conditions involving external oxidants and narrowed substrate scope remain to be substantially improved (see Figure S7 of the SI for a detailed comparison). Nevertheless, these early studies prompted us to investigate if our catalytic system involving a similar radical intermediate can be engineered to switch from dehydrogenation to γ-C−H lactonization, thereby realizing bimodal catalysis using a copper catalyst. When performing dehydrogenation of substrate **A29** under our standard reaction conditions, we observed the formation of a trace amount of

lactone **C29**. Hence, a series of experiments were conducted to favor the lactonization reaction pathway (Figure S8 of the SI). In particular, DCE suppressed the formation of lactone, while replacing the AcOH additive with a stronger acid such as TFA increased the yield of lactone. To our delight, when dioxane was used as the solvent and TFA was included as an additive, **C29** was formed in 78% yield with no **B29** detected. For substrates with unactivated γ-methylene C−H bonds, a combination of dioxane/nitromethane as solvent with $[(CH_3CN)_4Cu]BF_4$ was found to be optimal for lactonization (Figure S9 of the SI). Representative examples of this conditions-based switch in reactivity from dehydrogenation to lactonization are given in Fig. 3a (see Figure S10 of the SI for details). Selectivity for lactonization over dehydrogenation can be perfectly controlled for substrates bearing tertiary or benzylic γ-C−H bonds (e.g., **C27**-**C29**, **C35**, **C37**, **C38**, **C48**). Lactonization of long-chain fatty acids and amino acids with unactivated γ-methylene were also feasible via this method (e.g., **C43** and **C51**), though competing dehydrogenation was observed with these starting materials. Owing to the large differences between these two products, the rapid diversification of carboxylic acids could be envisioned because of this dual dehydrogenation/lactonization reactivity, which is valuable from the perspective of chemical space expansion.

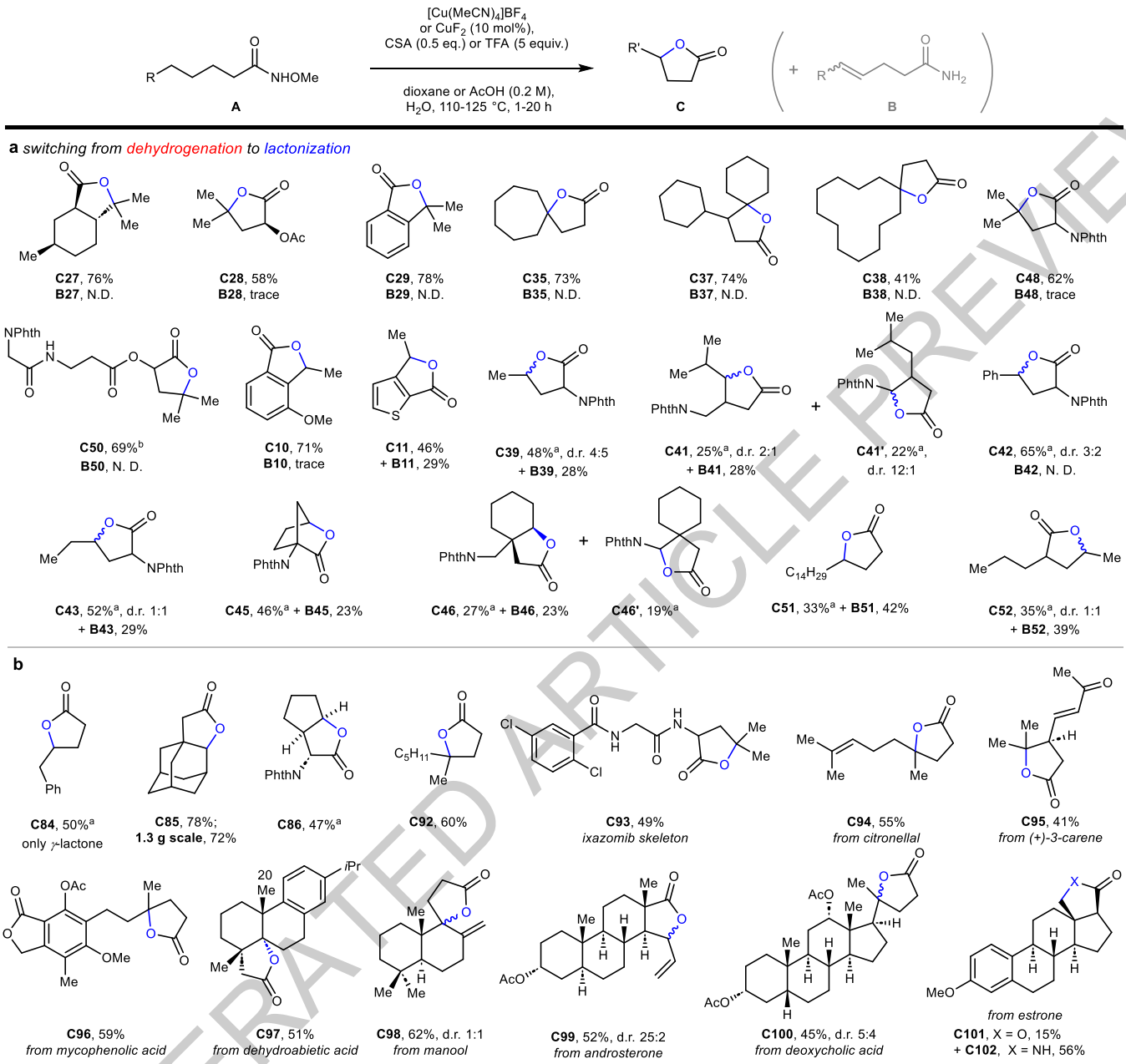

A variety of additional substrates were prepared to test the generality of the lactonization reaction (Fig. 3b and Extended Data Fig. 2). Activated benzylic, allylic, and propargylic γ-C–H bonds (Extended Data Fig. 2) generally underwent efficient lactonization regardless of whether the position was primary (**C68-C73**), secondary (**C74-C83**, **C87-C90**) or tertiary (**C91**). As noted above, substrates with unactivated secondary (**B84-C86**) and tertiary (**C92**) γ-C−H bonds (Fig. 3b) also performed well in the reaction. In the case of **C84**,

although a more reactive δ-benzylic site is present, γ-lactone is still exclusively formed via 1,5-H atom abstraction. As expected, the method displayed favorable functional group compatibility with synthetically valuable aryl halides (**C78**) and oxidatively sensitive groups such as olefins (**C81**, **C83**, and **C88**), alkynes (**C87** and **C88**), and highly electron rich arenes (**C74**), which are unlikely to be tolerated by conventional approaches that rely on strong external oxidants.

We next sought to examine the reliability and synthetic utility of the reaction by examining the lactonization of several derivatives of natural products and pharmaceuticals (**C93-C102**, Fig. 3b). As with the dehydrogenation, the γ-lactonization tolerated structural and functional complexity of these compounds well. Notably, when the *γ* position is blocked, the amidyl radical can instead abstract a *δ*-hydrogen, for example, affording rearranged product **C95** in 41% yield (see the SI for details). Interestingly, treatment of the derivative of estrone with the standard conditions gave the lactam as the main product (**C102**) with lactone **C101** as the minor product. This suggests that the reaction may proceed through a alkyl Cu(III) intermediate that undergoes C−N and C−O bond formation to avoid the unfavorable formation of an unstabilized primary carbocation. We are currently exploiting this pathway to construct lactams from *N*-methoxyamides.

Remarkably, simultaneous bimodal oxidation reactions at two different sites are also realized for diacid substrates (Fig. 4a), allowing for either dehydrogenation-lactonization (**BC102**), or dehydrogenation-lactamization (**BC103**) sequentially. It is noteworthy that our reactions were also efficient using low loading of catalyst with prolonged reaction time (Fig. 4b). Both dehydrogenation and lactonization proceeded smoothly with as low as 0.5 mol% of copper under an argon atmosphere, and the products were obtained in almost the same yields as when 10 mol% catalyst was used. In addition, our reactions can also proceed at

lower temperature (100 ˚C) with extended reaction time (see Figure S12 for details). A series of experiments were conducted to investigate the mechanism of the dehydrogenation and lactonization reactions (Extended Data Fig. 3). While screening the reaction conditions, we found that when 2,2'-biquinoline was added as a ligand, the reaction mixture turned an intense purple color rather than the usual blue or green (see Figure S14 of the SI for details). This is a characteristic of the formation of Cu(I)-biquinoline complex[36,27] and suggests that Cu(I) produced by disproportionation of the CuF_2 precatalyst is present in solution as a potential active catalyst[37]. A radical clock experiment was performed to investigate the radical intermediacy. When compound **A66** was subjected to the standard conditions, diene **B66** was obtained in 45% yield (Extended Data Fig. 3b). Presumably, the carbon-centered radical **Int-1** formed by 1,5-H-abstraction rearranged via an opening of the adjacent cyclopropane, forming the primary allylic radical **Int-2**, which can subsequently undergo oxidative elimination to afford diene **B66**. Taken together, these results support a mechanism initiated by Cu(I)-catalyzed oxidation of the *N*-methoxyamide to afford an amidyl radical, which then rearranges to a carbon-centered radical at the γ-position via 1,5-HAT.

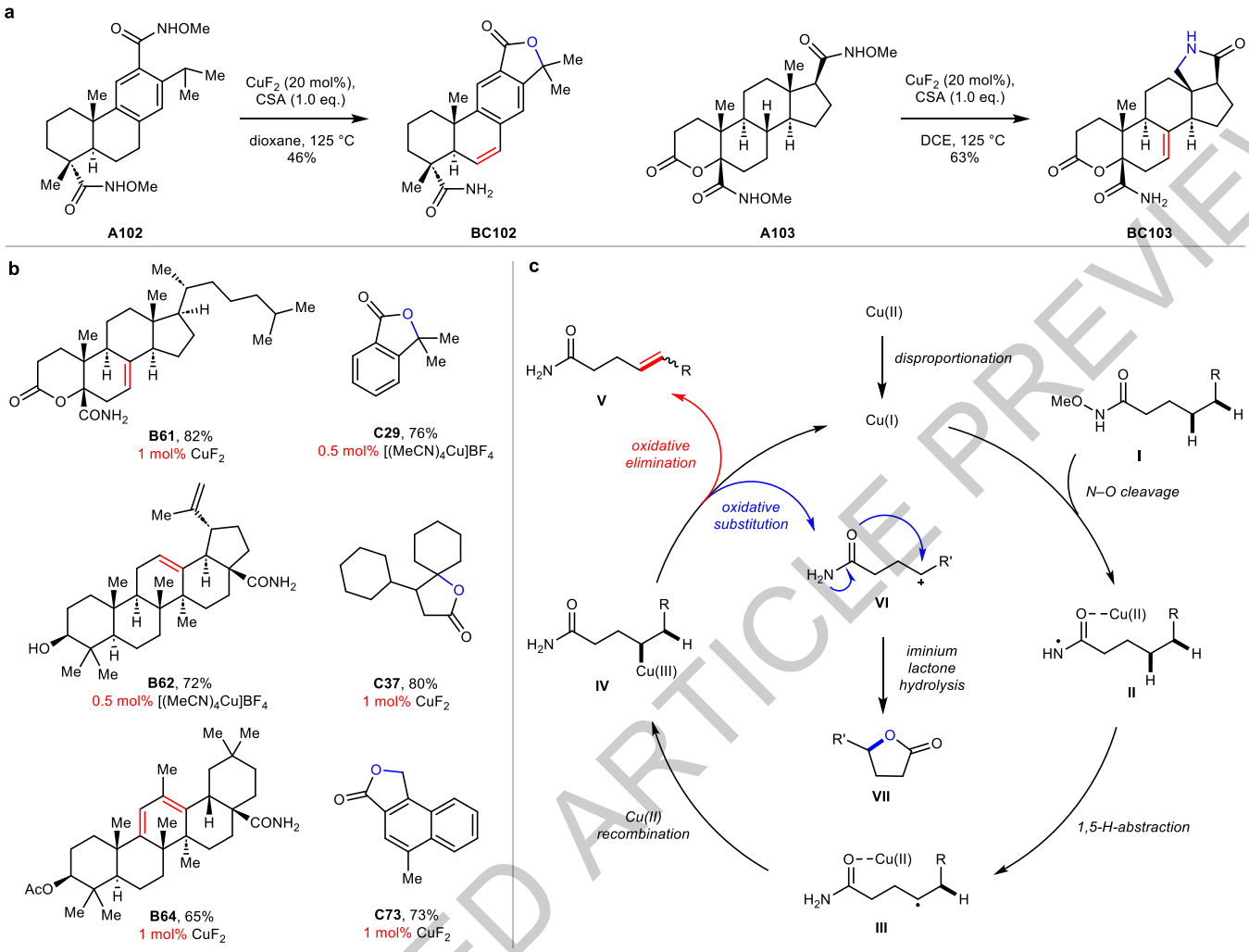

Based on Kochi's mechanistic studies on radical pathways with copper[30], we envision two plausible pathways of the elimination: 1) a Cu(II)-induced oxidation of the alkyl radical to a carbocation followed by a subsequent *β*-deprotonation; 2) a recombination of the alkyl radical and Cu(II) to form an alkylcopper(III) intermediate followed by a *β*-oxidative elimination. If the elimination proceeds through *β*-deprotonation, the more acidic *β*-H should be preferentially eliminated, which is contrary to the regioselectivity we observed. Furthermore, we treated alkyl chloride **A67** with $AgBF_4$ for in-situ carbocation generation (Extended Data Fig. 3c). Contrary to the regioselectivity of our reaction, this reaction afforded the β,γ- and γ,δ-olefins in a 10:1 mixture (Figure S16 of the SI). Thus, our copper-catalyzed dehydrogenation unlikely proceeds via a

cation intermediate, and the second pathway involving organocopper(III) species is more plausible[38]. In this scenario, the more hydridic H is preferentially eliminated (Figure S19 of the SI). In addition, the coordination of the amide to the copper(III) to form a metallocycle, favoring the elimination of an exocyclic δ-H rather than an endocyclic β-H[39], could also contribute to the γ,δ-selectivity. Kochi and coworkers revealed that the ratio of elimination to substitution of organocopper(III) intermediates was found to be largely controlled by nature of the substrate (with substrates that can form more stable carbocations typically favoring substitution), but also exhibited sensitivity to the reaction conditions[30], particularly copper sources and solvents (more polar solvents favor oxidative substitution). These findings are in line with our experimental data. Of note, **C68-C73**, **C85**, and **C101** rule out the possibility that the lactone is formed via a cyclization of the dehydrogenated amide under acidic conditions (Figure S17 of the SI).

Based on our experimental results and literature precedents, a proposed mechanism for this bimodal dehydrogenation/lactonization reaction is outlined in Fig. 4c. An in-situ generation of Cu(I) initiates the reaction by promoting the reductive cleavage of the N−O bond of *N*-methoxyamide **I** to form amidyl radical **II** and a Cu(II) species. Once formed, **II** undergoes 1,5-H atom abstraction to afford alkyl radical **III**, which could recombine with Cu(II) to form alkylcopper(III) intermediate **IV**, analogous to the Kharasch allylic oxidation[40]. From this point forward, the reaction diverges into two paths. On the one hand, alkylcopper(III) species have significant carbocationic character. Hence, they can undergo oxidative elimination to generate alkene **V**. On the other hand, in a more polar environment (with more polar solvent and a more acidic additive), the elimination may be suppressed, and instead, carbocation intermediate **VI** can form. Intramolecular trapping of cation **VI** and subsequent iminium hydrolysis provides lactone **VII**. Remarkably,

for substrates where the carbocationic intermediate **VI** is relatively stabilized (e.g., when the γ position is benzylic, tertiary, or allylic), the selectivity between the two pathways could be perfectly controlled.

In conclusion, we have developed a bimodal Cu-catalyzed dehydrogenation/lactonization of synthetically common *N*-methoxyamides. This redox-neutral process led to two controllable reaction pathways for synthesizing *γ,δ*-unsaturated primary amides and γ-lactones from various carboxylic acids (as the precursors of *N*-methoxyamides). Both the dehydrogenation and the lactonization could serve as strategies for the diversifications of a variety of drug molecules and natural products. Further development of the current methodology for the synthesis of lactams is underway in our laboratory.

Acknowledgements: We acknowledge The Scripps Research Institute, NIH (NIGMS, 2R01GM084019) for financial support. The content is solely our responsibility and does not necessarily represent the official views of the National Institutes of Health. We thank D. Strassfeld for proofreading and providing helpful suggestions in preparing the manuscript. We thank Z. Li and Y.-K. Lin for proofreading supplementary information and repeating reactions. We thank M. Gembicky and J. Bailey of the UCSD Crystallography Facility for X-ray crystallographic analysis. We thank D.-H. Huang, L. Pasternack, and G. Kroon of the Nuclear Magnetic Resonance Facility of the Scripps Researcher Services for their assistance with NMR analysis. We thank B. Webb and E. Billings of the Scripps Center for Metabolomics and Mass Spectrometry and Q. N. Wong of the Scripps Automated Synthesis Facility for assistance with mass spectrometry. This paper is dedicated to the memory of the late Dr. Dong-Hui, Wang.

Author contributions: J.-Q. Y. conceived the concept. S. Z. and Z.-J. Z. discovered and developed the dehydrogenation/lactonization reaction. S. Z. and Z.-J. Z. conducted the mechanistic studies. S. Z., Z.-J. Z. and J.-Q. Y. wrote the manuscript. J.-Q. Y. directed the project.

Competing interests: J.-Q.Y., S. Z., and Z.-J. Z. are inventors on a patent application related to this work (US Patent application 63/605,065) filed by The Scripps Research Institute. The authors declare no other competing interests.

Supplementary Information is available in the online version of the paper.

Data availability: Crystallographic data for compounds **B63**, **B64**, **C27**, **C86, C101,** and **C102**, as well as for derivatives of **B62** (labeled as **B62-ketone**) and **B65** (labeled as **B65-Ac**) are available in the Supplementary Information files and from the Cambridge Crystallographic Data Center under reference numbers CCDC 2279927, CCDC 2271734, CCDC 2271733, CCDC 2271730, CCDC 2271732, CCDC 2271731, CCDC 2296322, and CCDC 2296327, respectively. All other data supporting the findings of this study are available in the Article and its Supplementary Information files.

References:

1. Larock, R. C. *Comprehensive Organic Transformation* (Wiley, 2018).
2. Ishihara, Y. & Baran, P. S. Two-phase terpene total synthesis: historical perspective and application to the Taxol® problem. *Synlett* **12**, 1733−1745 (2010).
3. Qiu, Y. & Gao, S. Trends in applying C−H oxidation to the total synthesis of natural products. *Nat. Prod. Rep.* **33**, 562−581 (2016).
4. Buist, P. H. Fatty acid desaturases: selecting the dehydrogenation channel. *Nat. Prod. Rep.* **21**, 249−262 (2004).
5. Rettie, A. E., Rettenmeier, A. W., Howald, W. N. & Baillie, T. A. Cytochrome P-450-catalyzed formation of Δ^4-VPA, a toxic metabolite of valproic acid. *Science* **235**, 890−893 (1987).

6. Zhou, J. *et al.* Spectroscopic studies of substrate interactions with clavaminate synthase 2, a multifunctional a-KG-dependent non-heme iron enzyme: correlation with mechanisms and reactivities. *J. Am. Chem. Soc.* **123**, 7388−7398 (2001).

7. Cernak, T.; Dykstra, K. D.; Tyagarajan, S.; Vachal, P. & Krska, S. W. The medicinal chemist's toolbox for late stage functionalization of drug-like molecules. *Chem. Soc. Rev.* **45**, 546−576 (2016).

8. Blakemore, D. C. *et al.* Organic synthesis provides opportunities to transform drug discovery. *Nat. Chem.* **10**, 383−394 (2018).

9. Hong, B.; Luo, T. & Lei, X. Late-stage diversification of natural products. *ACS Cent. Sci.* **6**, 622−635 (2020).

10. Breslow, R. & Baldwin, S. W. Conversion of cholestanol to 12-oxocholestanol and to cholest-14-enol and-8(14)-enol by remote oxidation. *J. Am. Chem. Soc.* **92**, 732−734 (1970).

11. Breslow, R. Biomimetic chemistry and artificial enzymes: catalysis by design. *Acc. Chem. Res.* **28**, 146−153 (1995).

12. Groves, J. T.; Nemo, T. E. & Myers, R. S. Hydroxylation and epoxidation catalyzed by iron-porphine complexes. Oxygen transfer from iodosylbenzene. *J. Am. Chem. Soc.* **101**, 1032−1033 (1979).

13. Huang, X. & Groves, J. T. Beyond ferryl-mediated hydroxylation: 40 years of the rebound mechanism and C−H activation. *J. Biol. Inorg. Chem.* **22**, 185−207 (2017).

14. Kim, C.; Dong, Y. & Que, L. Jr. Modeling nonheme diiron enzymes: hydrocarbon hydroxylation and desaturation by a high-valent Fe_2O_2 diamond core. *J. Am. Chem. Soc.* **119**, 3635−3636 (1997).

15. Hull, J. F. *et al.* Manganese catalysts for C−H activation: an experimental/ theoretical study identifies the stereoelectronic factor that controls the switch between hydroxylation and desaturation pathways. *J. Am. Chem. Soc.* **132**, 7605−7616 (2010).

16. Bigi, M. A.; Reed, S. A. & White, M. C. Diverting non-haem iron catalyzed aliphatic C−H hydroxylations towards desaturations. *Nat. Chem.* **3**, 216−222 (2011).

17. Zhu, R.-Y.; Farmer, M. E., Chen, Y.-Q. & Yu, J.-Q. A simple and versatile amide directing group for C−H functionalizations. *Angew. Chem. Int. Ed.* **55**, 10578−10599 (2016).

18. Wang, D.-H.; Wasa, M. Giri, R. & Yu, J.-Q. Pd(II)-catalyzed cross-coupling of sp^3 C−H bonds with sp^2 and sp^3 boronic acids using air as the oxidant. *J. Am. Chem. Soc.* **130**, 7190−7191 (2008).

19. Zard, S. Z. Recent progress in the generation and use of nitrogen-centred radicals. *Chem. Soc. Rev.* **37**, 1603 (2008).

20. Fazekas, T. J.; Alty, J. W.; Neidhart, E. K.; Miller, A. S.; Leibfarth, F. A. & Alexanian, E. J. Diversification of aliphatic C−H bonds in small molecules and polyolefins through radical chain transfer. *Science* **375**, 545−550 (2022).

21. Davies, J.; Svejstrup, T. D.; Fernandez Reina, D. F.; Sheikh, N. S. & Leonori, D. Visible-light-mediated synthesis of amidyl radicals: transition-metal-free hydroamination and N-arylation reactions. *J. Am. Chem. Soc.* **138**, 8092−8095 (2016).

22. Davies, J.; Morcillo, S. P.; Douglas, J. J. & Leonori, D. Hydroxylamine derivatives as nitrogen-radical precursors in visible-light photochemistry. *Chem. - Eur. J.* **24**, 12154−12163 (2018).

23. Jin, W. & Yu, S. Photoinduced and palladium-catalyzed remote desaturation of amide derivatives. *Org. Lett.* **23**, 6931−6935 (2021).

24. Kwon, K.; Simons, R. T.; Nandakumar, M. & Roizen, J. L. Strategies to generate nitrogen-centered radicals that may rely on photoredox catalysis: development in reaction methodology and applications in organic synthesis. *Chem. Rev.* **122**, 2353−2428 (2022).

25. Bach, R. D. & Schlegel, H. B. The bond dissociation energy of the N−O bond. *J. Phys. Chem. A* **125**, 5014−5021 (2021).

26. Stateman, L. M.; Dare, R. M.; Paneque, A. N. & Nagib, D. A. Aza-heterocycles via copper-catalyzed, remote C−H desaturation of amines. *Chem* **8**, 210−224 (2022).

27. Faulkner, A.; Race, N. J.; Scottb, J. S. & Bower, J. F. Copper catalyzed Heck-like cyclizations of oxime esters. *Chem. Sci.* **5**, 2416−2421 (2014).

28. Kochi, J. K. The decomposition of peroxides catalyzed by copper compounds and the oxidation of alkyl radicals by cupric salts. *J. Am. Chem. Soc.* **85**, 1958−1968 (1963).

29. Kochi, J. K. Mechanisms of organic oxidation and reduction by metal complexes: electron and ligand transfer processes form the basis for redox reactions of radicals and metal species. *Science*, **155**, 415−424 (1967).

30. Kochi, J. K.; Bemis, A. & Jenkins, C. L. Mechanism of electron transfer oxidation of alkyl radicals by copper(II) complexes. *J. Am. Chem. Soc.* **90**, 4616−4625 (1968).

31. Barton, D. H. R.; Beckwith, A. L. J. & Goosen, A. Photochemical transformations. Part XVI. A novel synthesis of lactones. *J. Chem. Soc.* 181−190 (1965).

32. Neale, R. S.; Marcus, N. L. & Schepers, R. G. The chemistry of nitrogen radicals. IV. The rearrangement of N-halamides and the synthesis of iminolactones[1]. *J. Am. Chem. Soc.* **88**, 3051−3058 (1966).

33. Chen, K.; Richter, J. M. & Baran, P. S. 1,3-Diol synthesis via controlled, radical-mediated C−H functionalization. *J. Am. Chem. Soc.* **130**, 7247−7249 (2008).

34. Chen, K. & Baran, P. S. Total synthesis of eudesmane terpenes by site-selective C−H oxidations. *Nature*, **459**, 824−828 (2009).

35. Richers, J.; Heilmann, M.; Drees, M. & Tiefenbacher, K. Synthesis of lactones via C−H functionalization of nonactivated C(sp^3)−H bonds. *Org. Lett.* **18**, 6472−6475 (2016).

36. Hoste, J. On a new copper specific group. *Anal. Chim. Acta*, **4**, 23−27 (1950).

37. Ribas, X. *et al.* Aryl C−H activation by Cu^{II} to form an organometallic aryl-Cu^{III} species: a novel twist on copper disproportionation, *Angew. Chem. Int. Ed.* **41**, 2991−2994 (2002).

38. Xu, J. *et al.* Copper-catalyzed trifluoromethylation of terminal alkenes through allylic C−H bond activation. *J. Am. Chem. Soc.* **133**, 15300−15303 (2011).

39. Wu, X.; Riedel, J. & Dong, V. M. Transforming olefins into γ,δ-unsaturated nitriles through copper catalysis. *Angew. Chem. Int. Ed.* **56**, 11589−11593 (2017).

40. Beckwith, A. L. J. & Zavitsas, A. A. Allylic oxidations by peroxy esters catalyzed by copper salts. The potential for stereoselective syntheses. *J. Am. Chem. Soc.* **108**, 8230−8234 (1986).

Fig. 1: Bimodal oxidation via a common radical intermediate. (a) Nature's approach: hepatic P450-mediated bimodal oxidation of valproic acid. **(b)** Our design of Cu-catalyzed bimodal oxidation of *N*-methoxyamides via a common alkyl radical intermediate. **(c)** Synthetic approach: dual desaturation/lactonization reactivity enables rapid diversification of carboxylic acids.

Fig. 2: Substrate scope for the dehydrogenation reaction. Reaction conditions: **A** (0.1 mmol), CuF_2 (10 mol%), AcOH (8 eq.) or CSA (0.5 eq.), dioxane (0.50 mL), at 100-125 °C for 1-20 h (see the SI for details). Isolated yields are reported. [a]**L** (20 mol%) was added. [b]The solvent is DCE. [c]The acid is $TsOH•H_2O$ (0.5 eq.). [d]$[(MeCN)_4Cu]BF_4$ (10 mol%) was used instead of CuF_2. rr is the ratio of γ,δ-alkene/β,γ-alkene.

Fig. 3: Substrate scope for the lactonization reaction. (a) Representative examples of bimodal dehydrogenation/lactonization, see Figure S10 of the SI for details. **(b)** More substrates for the lactonization. Reaction conditions: **A** (0.1 mmol), CuF_2 (10 mol%) or $[(CH_3CN)_4Cu]BF_4$ (10 mol%), acid (5 eq. TFA or 0.5 eq. CSA), dioxane or AcOH (0.50 mL), at 125 °C for 1-20 h (see the SI for details). Isolated yields are reported. [a]The solvent is dioxane/$MeNO_2$ (0.25 mL/0.25 mL). [b]0.5 eq. $TsOH•H_2O$ was used. d.r. = diastereomer ratio, see the SI for details.

Fig. 4: Reactions of diacid derivatives or using a low loading of copper and plausible mechanism. (a) Simultaneous bimodal oxidations within complex systems. L: dehydrogenation-lactonization; R: dehydrogenation-lactamization. **(b)** Experiments using a low loading of copper. Reaction conditions for dehydrogenation: **A** (0.1 mmol), catalyst (0.5-1 mol%), CSA (0.5 eq), dioxane (0.50 mL), 125 °C, 20-24 h. Reaction conditions for lactonization: **A** (0.1 mmol), catalyst (0.5-1 mol%), TFA (5 eq), dioxane or AcOH

(0.50 mL), 125 °C, 24 h. See the SI for details. Isolated yields are reported. **(c)** Plausible mechanism based on the mechanistic studies and literature precedents.

Extended Data Fig. 1: Continued Substrate scope for the dehydrogenation reaction. Reaction conditions: **A** (0.1 mmol), CuF_2 (10 mol%), AcOH (8 eq.) or CSA (0.5 eq.), dioxane (0.50 mL), at 100-125 °C for 2-20 h (see the SI for details). Isolated yields are reported. [a]**L** (20 mol%) was added. [b]The solvent is DCE. rr is the ratio of γ,δ-alkene/β,γ-alkene.

Extended Data Fig. 2: Continued substrate scope for the lactonization reaction. Reaction conditions: **A** (0.1 mmol), CuF_2 (10 mol%) or $[(CH_3CN)_4Cu]BF_4$ (10 mol%), TFA (5 eq.), dioxane (0.50 mL), at 125 °C for 1-20 h (see the SI for details). Isolated yields are reported. [a]The solvent is dioxane/$MeNO_2$ (0.25 mL/0.25 mL). [a]The acid is $TsOH•H_2O$ (1 eq.). [b]0.5 eq. CSA was used. [c]2.5 eq. TFA was used. d.r. = diastereomer ratio, see the SI for details.

Extended Data Fig. 3: Mechanistic studies. (a) Investigation of Cu(I) generated in-situ. **(b)** Radical clock experiment. **(c)** Inverted regioselectivity of elimination from a cationic intermediate. See the SI for details.

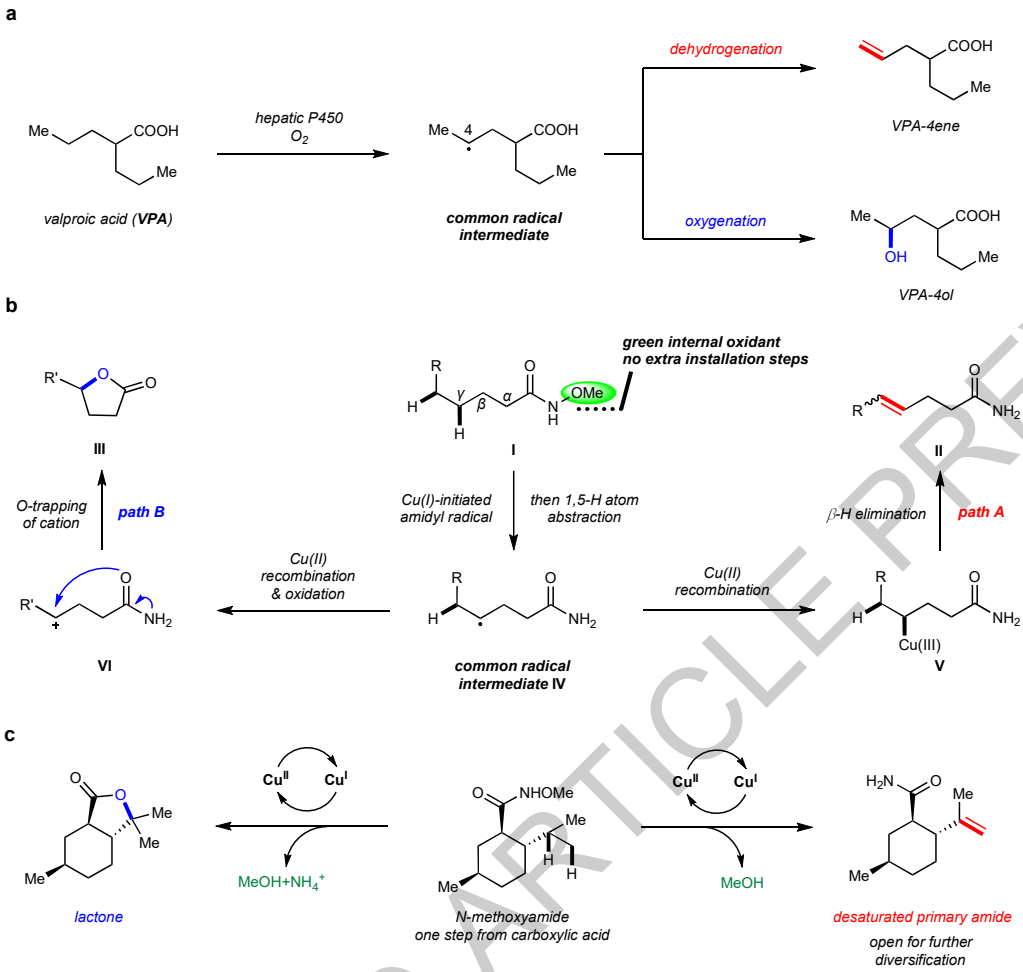

√controllable bimodal oxidation √redox-neutral √inexpensive catalyst √high regioselectivity √good functional group tolerance √readily available and stable substrates, >120 examples

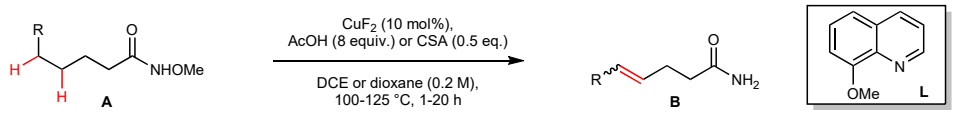

secondary

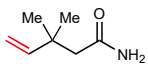

B1, 80%[a]

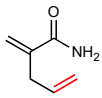

B2, 56%[a]

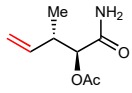

B3,75%[a,b]

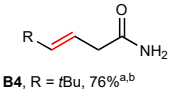

B4, R = *t*Bu, 76%[a,b]
B5, R = 1-admantyl, 72%[a,b]

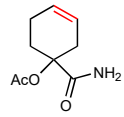

B6, 52%[a,b]

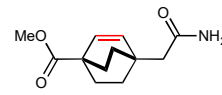

B7, 78%[a,b]

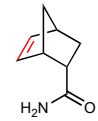

B8, 80%[a,b]

tertiary

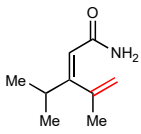

B26, 60%[c]

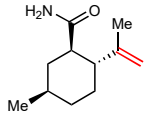

B27, 70%[a]

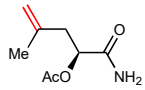

B28, 72%[a,b]

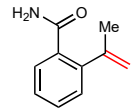

B29, 60%[b]

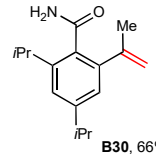

B30, 66%[b]

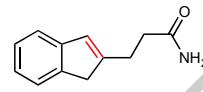

B31, 85%[a]

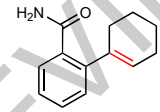

B32, 62%[b]

natural products and drugs

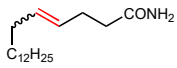

B51, 62%, 12:1 rr, 3:2 E/Z
from stearic acid

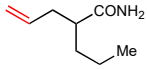

B52, 74%, 6:1 rr
from valproic acid

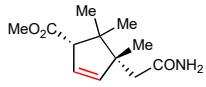

B53, 67%
from camphoric acid

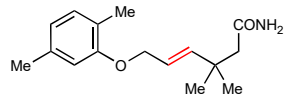

B54, 66%[b]
from gemfibrozil

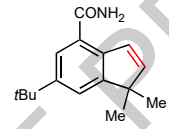

B55, 53%[b]
from celestolide

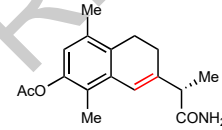

B56, 90%[b]
from santonin

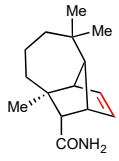

B57, 80%[a,b]
from isolongifolic acid

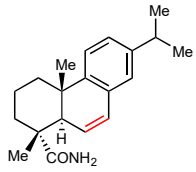

B58, 73%[b]; **1.6 g scale**, 72%
from dehydroabietic acid

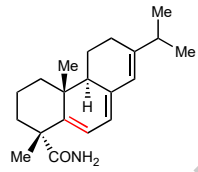

B59, 40%
from abietic acid

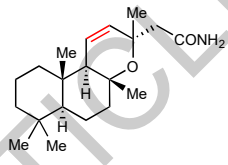

B60, 72%[a,b]
from (+)-manoyl oxide

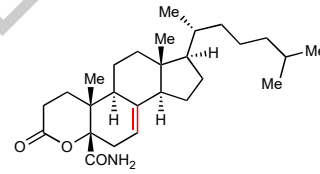

B61, 84%
from cholest-4-en-3-one

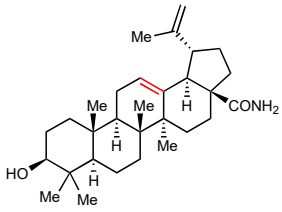

B62, 79%[d]
from betulinic acid

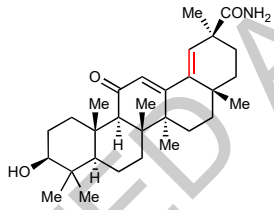

B63, 70%
from 18β-glycyrrhetinic acid

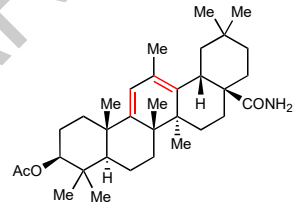

B64, 66%
from oleanic acid

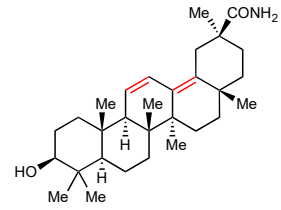

B65, 65%
from 18β-glycyrrhetinic acid

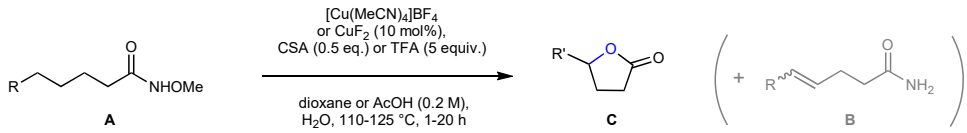

a *switching from dehydrogenation to lactonization*

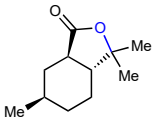

C27, 76%
B27, N.D.

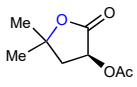

C28, 58%
B28, trace

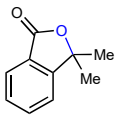

C29, 78%
B29, N.D.

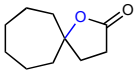

C35, 73%
B35, N.D.

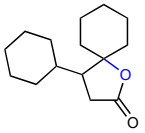

C37, 74%
B37, N.D.

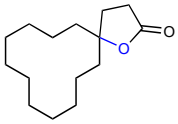

C38, 41%
B38, N.D.

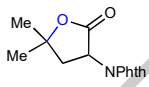

C48, 62%
B48, trace

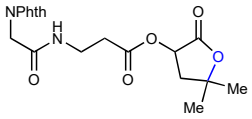

C50, 69%[b]
B50, N. D.

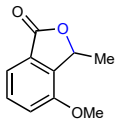

C10, 71%
B10, trace

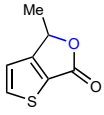

C11, 46%
+ **B11**, 29%

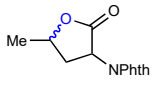

C39, 48%[a], d.r. 4:5
+ **B39**, 28%

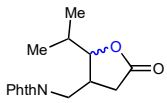

C41, 25%[a], d.r. 2:1
+ **B41**, 28%

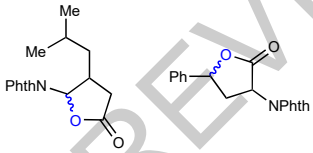

C41', 22%[a],
d.r. 12:1

C42, 65%[a], d.r. 3:2
B42, N. D.

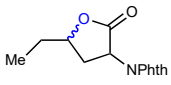

C43, 52%[a], d.r. 1:1
+ **B43**, 29%

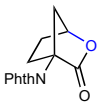

C45, 46%[a] + **B45**, 23%

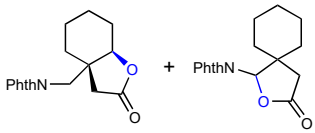

C46, 27%[a] + **B46**, 23%
C46', 19%[a]

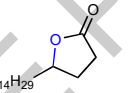

C51, 33%[a] + **B51**, 42%

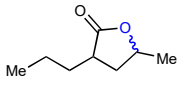

C52, 35%[a], d.r. 1:1
+ **B52**, 39%

b

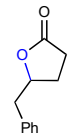

C84, 50%[a]
only γ-lactone

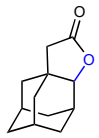

C85, 78%;
1.3 g scale, 72%

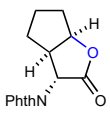

C86, 47%[a]

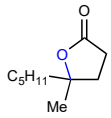

C92, 60%

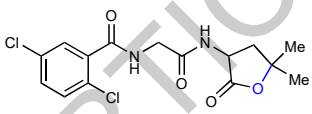

C93, 49%
ixazomib skeleton

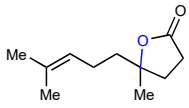

C94, 55%
from citronellal

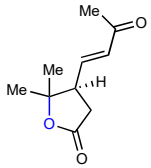

C95, 41%
from (+)-3-carene

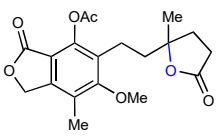

C96, 59%
from mycophenolic acid

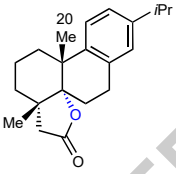

C97, 51%
from dehydroabietic acid

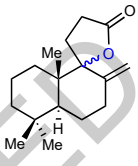

C98, 62%, d.r. 1:1
from manool

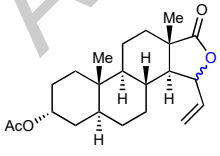

C99, 52%, d.r. 25:2
from androsterone

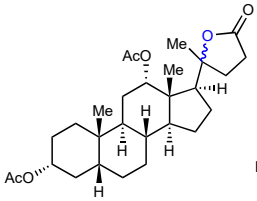

C100, 45%, d.r. 5:4
from deoxycholic acid

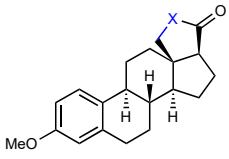

from estrone
C101, X = O, 15%
+ **C102**, X = NH, 56%

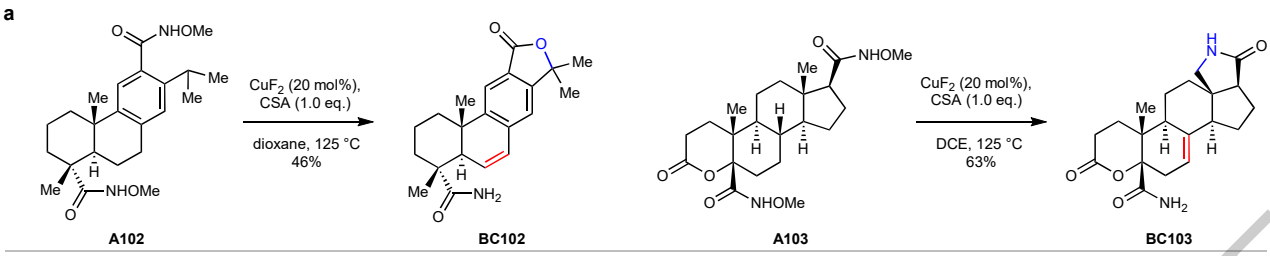

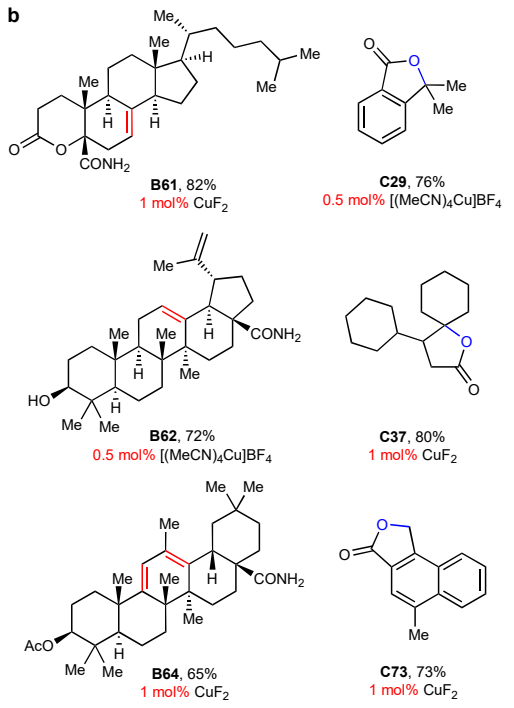

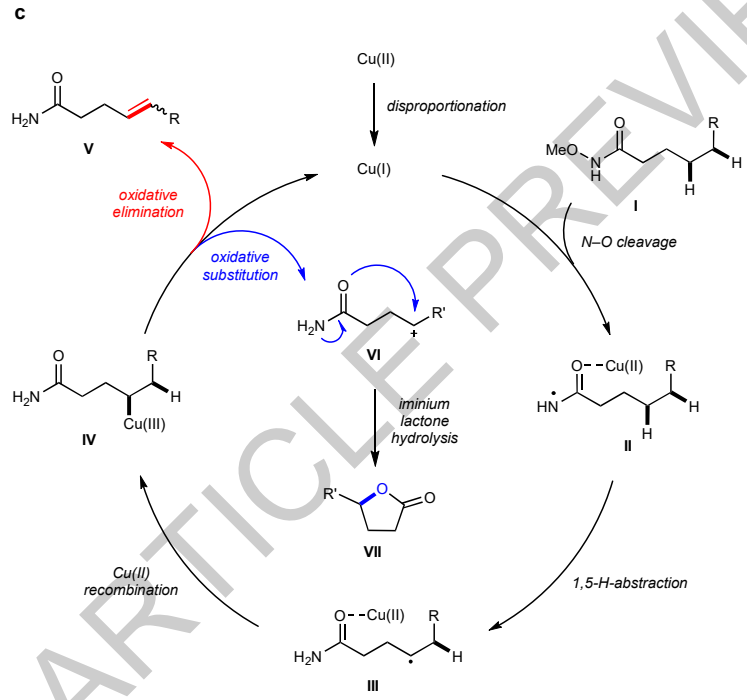

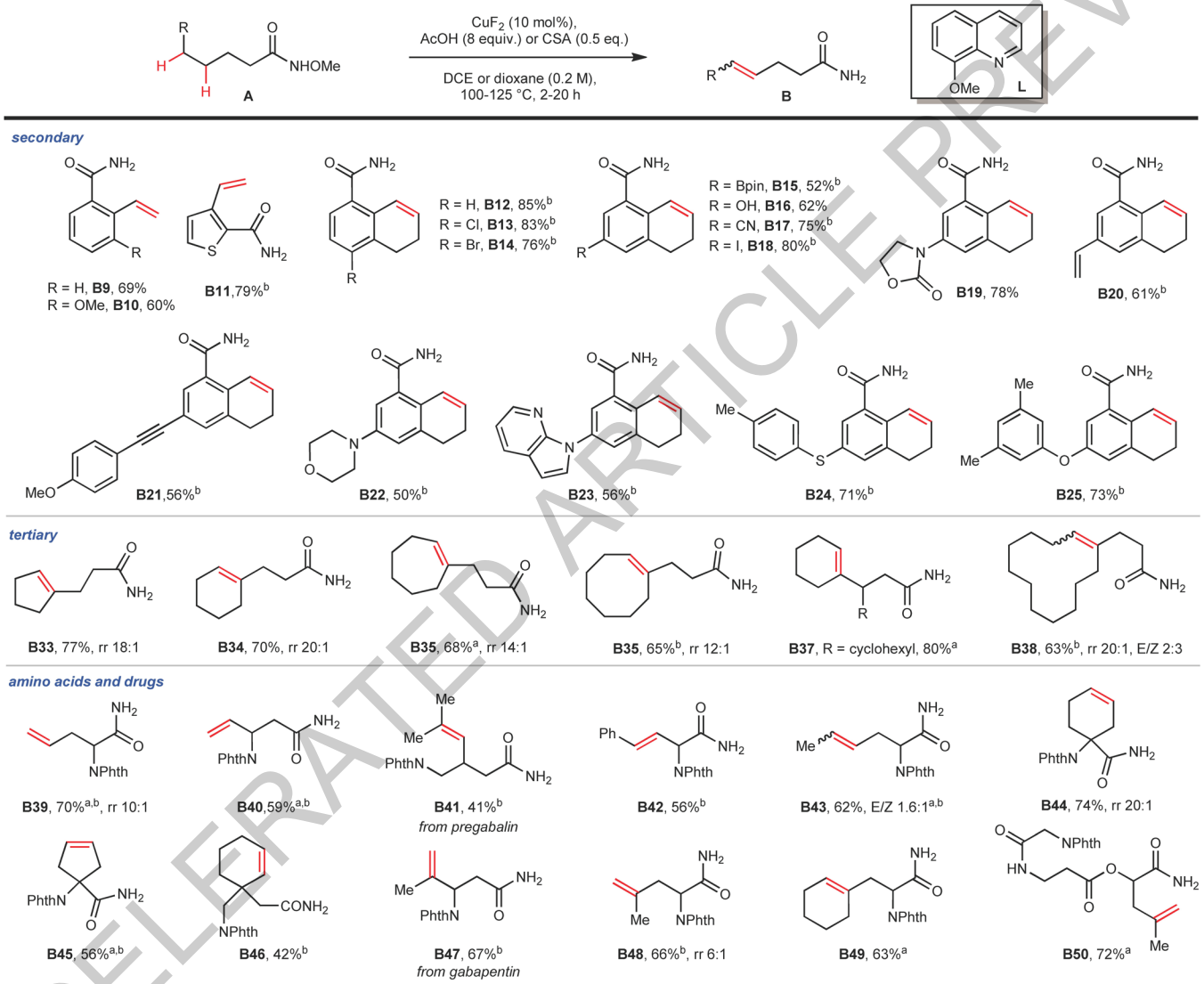

Extended Data Fig. 1

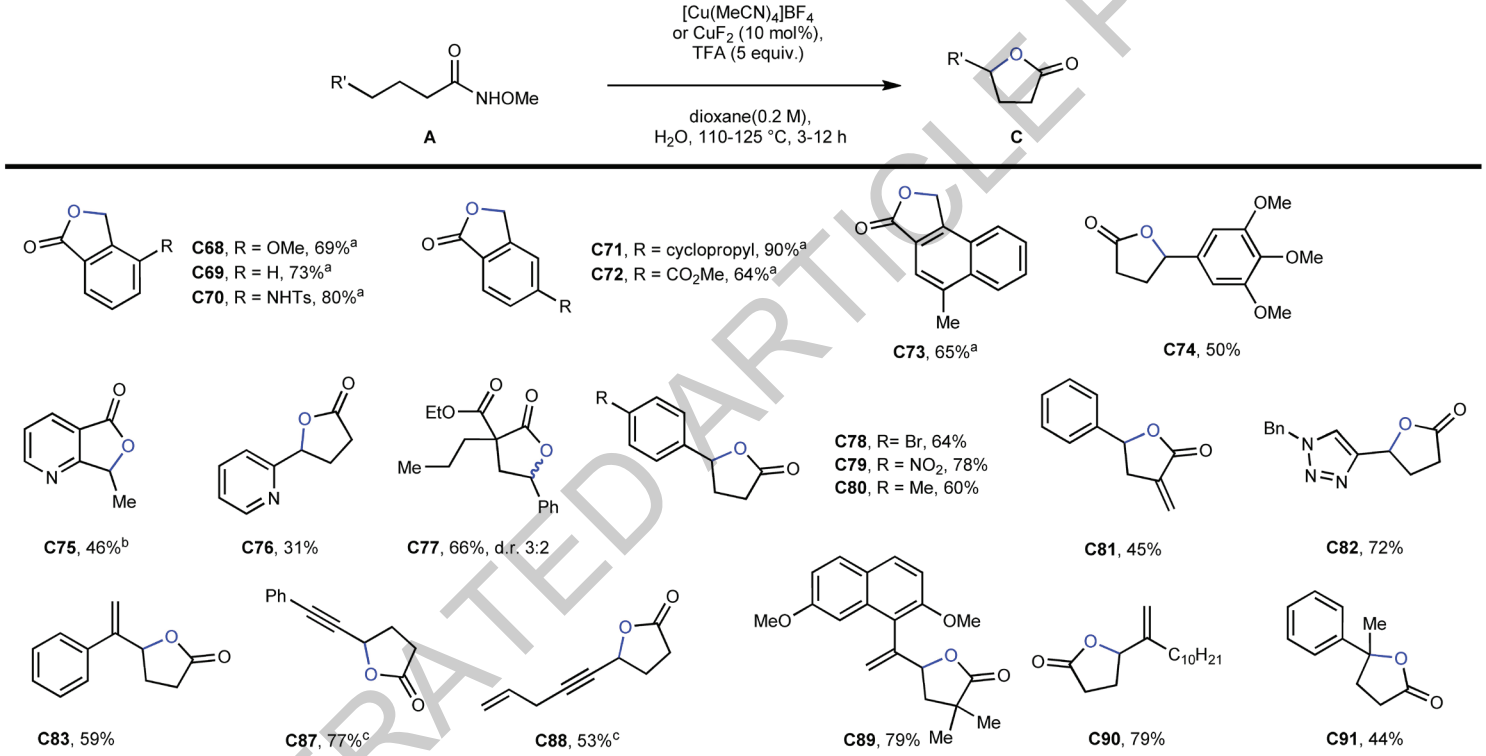

Extended Data Fig. 2

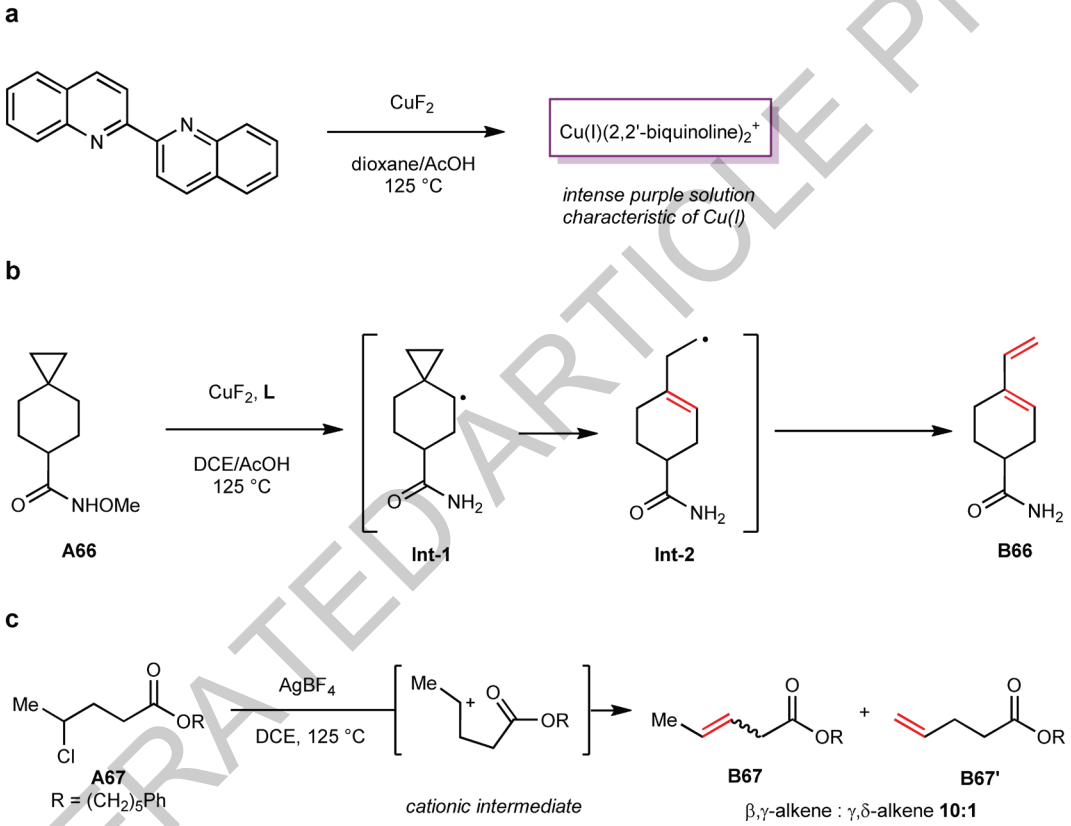

Extended Data Fig. 3